


RESEARCH ARTICLE

Continuous monitoring of postirradiation reoxygenation and cycling hypoxia using electron paramagnetic resonance imaging

Tatsuya Kawai^{1,2}  | Masayuki Matsuo^{3,4} | Yoichi Takakusagi^{3,5} | Keita Saito³ | Fuminori Hyodo^{3,6} | Nallathamby Devasahayam³ | Shingo Matsumoto^{3,7} | Shun Kishimoto³ | Hironobu Yasui^{3,8} | Kazutoshi Yamamoto³ | Murali C. Krishna³

¹Radiation Oncology Branch, National Cancer Institute, Bethesda, Maryland, USA

²Department of Radiology, Nagoya City University Graduate School of Medical Sciences, Nagoya, Japan

³Radiation Biology Branch, National Cancer Institute, Bethesda, Maryland, USA

⁴Department of Radiology, Gifu University, Gifu, Japan

⁵Institute for Quantum Life Science, National Institutes for Quantum Science and Technology, Chiba-city, Japan

⁶Department of Radiology, Frontier Science for Imaging, Gifu University, Gifu, Japan

⁷Division of Bioengineering and Bioinformatics, Graduate School of Information Science and Technology, Hokkaido University, Hokkaido, Japan

⁸Laboratory of Radiation Biology, Department of Applied Veterinary Sciences, Faculty of Veterinary Medicine, Hokkaido University, Hokkaido, Japan

Correspondence

Masayuki Matsuo, Department of Radiology, Gifu University, 1-1 Yanagido, Gifu, 501-1194, Japan.

Email: matsuo_m@gifu-u.ac.jp

Funding information

National Institutes of Health, USA; Grant number: 1ZIABC11692 SPS KAKEN Grants-in-Aid for Scientific Research; Grant number: 20H03628 and 20KK0253.

Reoxygenation has a significant impact on the tumor response to radiotherapy. With developments in radiotherapy technology, the relevance of the reoxygenation phenomenon in treatment efficacy has been a topic of interest. Evaluating the reoxygenation in the tumor microenvironment throughout the course of radiation therapy is important in developing effective treatment strategies. In the current study, we used electron paramagnetic resonance imaging (EPRI) to directly map and quantify the partial oxygen pressure (pO_2) in tumor tissues. Human colorectal cancer cell lines, HT29 and HCT116, were used to induce tumor growth in female athymic nude mice. Tumors were irradiated with 3, 10, or 20 Gy using an x-ray irradiator. Prior to each EPRI scan, magnetic resonance imaging (MRI) was performed to obtain T2-weighted anatomical images for reference. The differences in the mean pO_2 were determined through two-tailed Student's *t*-test and one-way analysis of variance. The median pO_2 60 min after irradiation was found to be lower in HCT116 than in HT29 (9.1 ± 1.5 vs. 14.0 ± 1.0 mmHg, $p = 0.045$). There was a tendency for delayed and incomplete recovery of pO_2 in the HT29 tumor when a higher dose of irradiation (10 and 20 Gy) was applied. Moreover, there was a dose-dependent increase in the hypoxic areas ($pO_2 < 10$ mmHg) 2 and 24 h after irradiation in all groups. In addition, an area that showed pO_2 fluctuation between hypoxia and normoxia ($pO_2 > 10$ mmHg) was also identified surrounding the region with stable hypoxia, and it slightly enlarged after recovery from acute hypoxia. In conclusion, we demonstrated the reoxygenation phenomenon in an *in vivo* xenograft model study using EPRI. These findings may lead to new knowledge regarding the reoxygenation process and possibilities of a new radiation therapy concept, namely, reoxygenation-based radiation therapy.

Abbreviations used: ANOVA, analysis of variance; EPRI, electron paramagnetic resonance imaging; FLASH, fast low-angle shot; FOV, field of view; MRI, magnetic resonance imaging; pO_2 , partial oxygen pressure; SEM, standard error of the mean.

Tatsuya Kawai and Masayuki Matsuo contributed equally to this study.

This is an open access article under the terms of the [Creative Commons Attribution-NonCommercial](https://creativecommons.org/licenses/by-nc/4.0/) License, which permits use, distribution and reproduction in any medium, provided the original work is properly cited and is not used for commercial purposes.

© 2022 The Authors. *NMR in Biomedicine* published by John Wiley & Sons Ltd.

KEYWORDS

cycling hypoxia, electron paramagnetic resonance imaging, radiation therapy, reoxygenation, tumor hypoxia

1 | INTRODUCTION

Although many chemical compounds and pharmacologic agents that modify the biological effect of ionizing radiation have been discovered, oxygen remains the most potent radiosensitizer.¹ Many solid tumors have been shown to contain subpopulations of hypoxic cells that limit the efficacy of cancer therapy, such as radiation, chemotherapy, and even surgery.^{2,3} Reoxygenation is critical in the conventional theory of multifractionated radiation therapy. A fraction of the previously hypoxic cells is aerated and made radiosensitive through a series of fractionated irradiation.^{2,3} In the tumor system used by van Putten and Kallman,⁴ the proportion of aerated hypoxic cells recovered to the pretreatment level within 24 h following delivery of fractionated dosage. Other studies showed that some tumors were reoxygenated within only 1 h, whereas other tumors took several days to be reoxygenated.^{5,6} The first component of reoxygenation, which is completed within hours, is attributed to the reopening of the tumor blood vessels that had temporarily closed immediately after irradiation. In this process, oxygen is redistributed in a region close enough to the capillary bed for the tumor cells to obtain sufficient oxygen in the normal state but at the same time distant enough to be aerated when the blood perfusion drops after irradiation.⁷ In addition to diffusion-limited chronic hypoxia, tumors also experience intermittent oxygen depletion known as acute or cycling hypoxia.^{8,9} Previous reports suggested that cycling hypoxia plays a key role in the resistance to therapies and tumor progression in preclinical experiments; however, the precise mechanism of this phenomenon and its clinical relevance remain unclear.¹⁰⁻¹² Investigating the mechanism of hypoxia in the tumor tissue during radiation therapy is thus important.

Electron paramagnetic resonance imaging (EPRI) is a spectroscopic technique similar to nuclear magnetic resonance imaging (MRI) that enables direct monitoring of the partial oxygen pressure (pO₂) in a tumor on a quantitative basis through the detection of the resonances of injected nontoxic stable paramagnetic free radicals with unpaired electrons.^{13,14} In previous studies, electron paramagnetic resonance oximetry revealed advantages in measuring pO₂ fluctuation and reoxygenation in tumor tissues after x-ray irradiation.¹⁵⁻¹⁷ Although these investigations employed single-point measurements that were limited in depicting the spatial distribution of pO₂ and its heterogeneity, mapping the oxygen tension in live animal tissues has also been explored.¹⁸ Matsumoto et al.¹⁹ and Yasui et al.²⁰ illustrated the presence of specific regions in tumors that showed fluctuations in oxygen concentrations in mouse models by using EPRI. In the current study, using *in vivo* murine models, oxygen distribution in the tumor was chronologically quantified, and the postirradiation reoxygenation profiles along with the phenomenon of cycling hypoxia were demonstrated using the EPRI technique, suggesting its potential use in the assessment of reoxygenation after each fraction of radiation therapy.

2 | MATERIALS AND METHODS

The study protocol was approved by the National Cancer Institute Animal Care and Use Committee (NCI-CCR-ACUC [Bethesda], Protocol# RBB-159). All procedures were performed in compliance with the Guide for the Care and Use of Laboratory Animal Resources (National Research Council, 1996).

2.1 | Animal experiment and tumor implantation

Two different human colon cancer cell lines, HT29 and HCT116, were tested in April 2013 by IDEXX RADIL (Columbia, MO, USA) using a panel of microsatellite markers and were subsequently authenticated. Female athymic nude mice were supplied by the Frederick National Laboratory for Cancer Research Center (Frederick, MD, USA). HT29 and HCT116 solid tumors were induced by subcutaneous injection of 5×10^5 cells in 50 μ l of phosphate buffer saline into the right hind leg, as described previously.²⁰ The experiments were initiated when tumors grew to approximately 600 to 700 mm³. The tumor size was measured externally using a caliper, and the volume was calculated using the following approximation formula: tumor volume = length \times width \times height \times 3.14 \times (1/6). The body weights measured before the experiments ranged from 21 to 27 g.

In the EPRI and MRI procedures, mice were anesthetized by isoflurane inhalation (4% for induction and 1.5% for maintaining anesthesia) in medical air (750 ml/min) and placed in the prone position with their tumor-bearing legs inside the resonator. During the examination, the respiratory rate of each mouse was monitored with a pressure transducer (SA Instruments Inc., NY, USA) and maintained at 60 ± 10 breaths per min. Core body temperature was monitored using a FISO FTI-10 temperature sensor (FISO Technologies Inc., Quebec, Canada) and maintained at

36 ± 1°C with a flow of warm air (EPRI) or water (MRI). For the administration of OX063, a 30-gauge needle was cannulated into the tail vein and extended using polyethylene tubing.

2.2 | EPRI for pO₂ monitoring

Technical details of the EPR scanner and oxygen image reconstruction are described in earlier reports.^{18,19} After the animal was placed in the resonator, the resonator (17 mm in diameter and 17 mm long) was used as an identical coil for EPRI and MRI operating at 300 MHz. Prior to each EPRI scan, MRI was performed to obtain T2-weighted anatomical images using a 7-T MRI scanner (Bruker BioSpin MRI GmbH, Billerica, MA, USA). Briefly, after a quick assessment of the sample position using a fast low-angle shot (FLASH) pilot sequence, T2-weighted axial and coronal images were obtained using a fast spin-echo sequence (RARE) with an echo time of 13 ms, repetition time of 2500 ms, 16 slices, RARE factor 8, and a resolution of 0.125 × 0.125 mm². For the convenience of coregistration with EPRI, all MR images had the same field of view (FOV) of 32 mm and a slice thickness of 2 mm. For the EPRI experiment, triarylmethyl (methyl-tris[8-carboxy-2,2,6,6-tetrakis[2-hydroxyethyl]-benzo [1,2-d:4,5-d']bis[1,3]dithiol-4-yl] trisodium salt; OX063, GE Healthcare) was injected intravenously through a cannula placed in the tail vein. To maintain the blood concentration, OX063 was administered as a 1.125 mmol/kg bolus injection followed by a 0.04 mmol/kg/min continuous injection. EPR signals were acquired following the radiofrequency excitation pulses (60 ns, 80 W, 70° flip angle using an analog-digital converter; 200 M samples/s). The spatial resolution of pO₂ images measured using EPRI was 1.8 mm, although the pixel resolution was digitally enhanced to coregister with MRI images. The scanning slice for EPRI was selected to include the tumor with the largest diameter in the coronal section (parallel to the longitudinal axis of the femur). Each pO₂ scanning was started 3 min after the OX063 injection, followed by a 3-min EPRI acquisition. For the cycling hypoxia experiments, continuous acquisitions were performed every 3 min. Thereafter, the images obtained from EPRI and MRI were coregistered using a code written in MATLAB (MathWorks) script, as previously described.^{18,19}

2.3 | Definitions of chronic and cycling hypoxia

Because there is no established definition of cycling hypoxia, the cycling hypoxia in this study was defined as pixels on EPRI, where the change in pO₂ was greater than or equal to three times 10 mmHg in the timeframe of continuous acquisition. Chronic hypoxia was defined as pixels that continuously demonstrated less than 10 mmHg.

2.4 | X-ray irradiation

The tumor-bearing mice were restrained without anesthesia in a custom-made jig to limit the radiation to the tumor-bearing leg. Tumors were irradiated with 3, 10, or 20 Gy using an x-ray irradiator, XRAD-320 (Precision X-ray Inc., North Branford, CT, USA), with a set voltage and current of 300 kV and 10 mA, respectively, at a dose rate of 2.16 Gy/min.

2.5 | Statistical analysis

All results are expressed as mean ± standard error of the mean (SEM). The differences among the means of groups were determined through two-tailed Student's *t*-test and one-way analysis of variance (ANOVA) using Prism 6 (GraphPad Software, CA, USA); *p* values less than 0.05 were considered statistically significant.

3 | RESULTS

3.1 | Effect of dosage on transient hypoxia in HT29 tumor

After pO₂ imaging prior to radiation treatment, the subcutaneous HT29 tumor was irradiated with 3, 10, or 20 Gy, followed by periodic EPRI examinations at 30 min, 60 min, 2 h, 18 h, 24 h, and 30 h after irradiation (Figure 1A). A continuous decrease in median pO₂ was observed from 30 to 60 min after irradiation in all groups. The minimum median pO₂ was 11.4 ± 0.9 mmHg in the 20-Gy group 2 h after irradiation, which was significantly lower than that in the 3- and 10-Gy groups (*p* < 0.01). There was a tendency for delayed and incomplete recovery of pO₂ in the tumor when a higher dose of irradiation (10 and 20 Gy) was applied. The median pO₂ 24 h after irradiation in the 10- and 20-Gy groups was

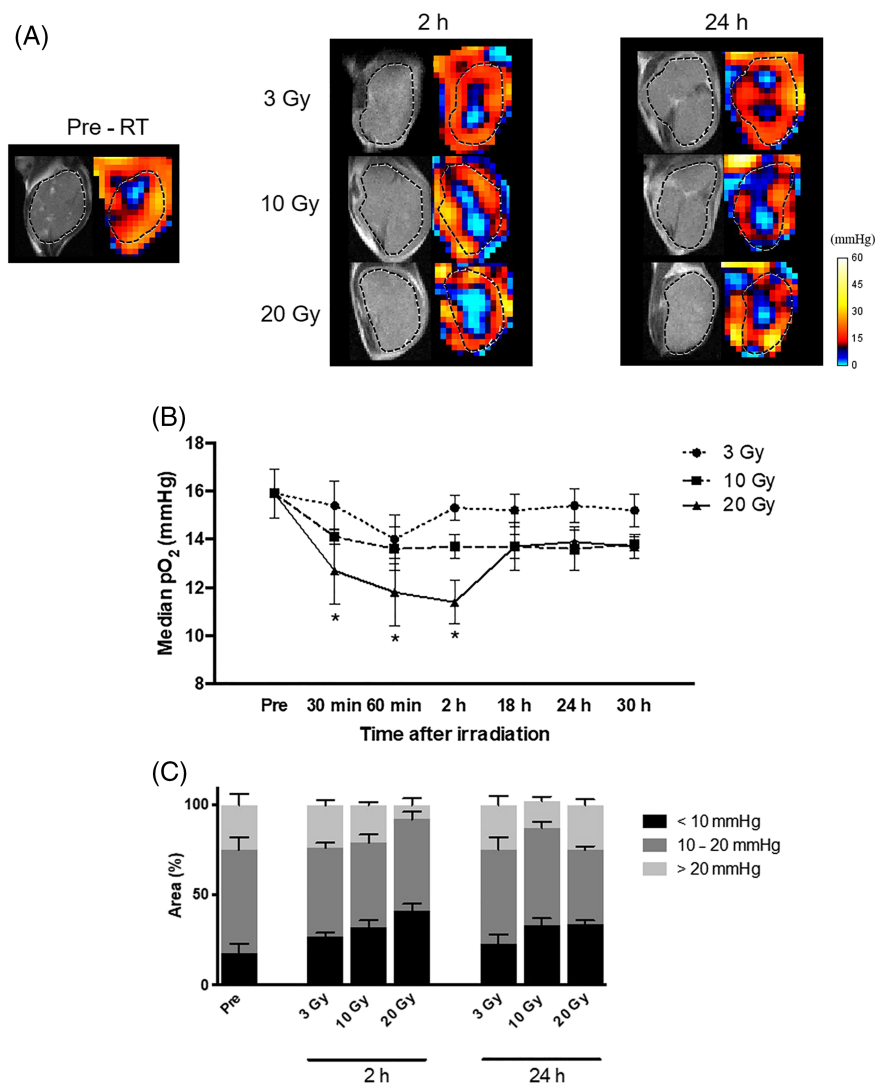


FIGURE 1 Dose effect on transient hypoxia in HT29 tumor. (A) Subcutaneous HT29 tumors ($n = 5$ in each group) were imaged before and after 3-, 10-, or 20-Gy irradiation on T2-weighted MR imaging (left) and electron paramagnetic resonance imaging (right) at 30 min, 60 min, 2 h, 18 h, 24 h, and 30 h. Representative images at preirradiation, 2 h after, and 24 h after are shown. The tumors are outlined with black dotted lines. (B) A continuous decrease in median partial oxygen pressure (pO_2) was observed in all groups from 30 to 60 min after irradiation. The median pO_2 at 2 h in the 20-Gy group was significantly lower than that in the 3- or 10-Gy group ($p < 0.01$). Delayed and insufficient pO_2 recovery was observed in the high-dose (10- and 20-Gy) groups. The median pO_2 at 24 h was significantly lower in the 10- and 20-Gy groups compared with that before irradiation ($p < 0.05$). (C) There was a dose-dependent increase in the hypoxic areas ($pO_2 < 10$ mmHg) 2 and 24 h after irradiation in all the groups. Although there was no significant difference in the hypoxic area between the 10- and 20-Gy groups 24 h after irradiation ($33\% \pm 4\%$ and $34\% \pm 3\%$, respectively), it was significantly smaller in the 3-Gy group ($23\% \pm 4\%$) than in the high-dose groups. *, statistically significant; RT, radiation therapy

significantly lower compared with that before irradiation (86.8% and 91.3%; $p = 0.010$ and $p = 0.014$, respectively; Figure 1B). There was a dose-dependent increase in the hypoxic areas ($pO_2 < 10$ mmHg) 2 and 24 h after irradiation in all groups. There was no significant difference in the hypoxic area between the 10- and 20-Gy groups 24 h after irradiation ($33\% \pm 4\%$ and $34\% \pm 3\%$, respectively). However, the increase in the hypoxic area was significantly smaller in the 3-Gy group ($23\% \pm 4\%$) than in the other two groups (Figure 1C).

3.2 | Strain-dependent difference in transient hypoxia between HT29 and HCT116 tumors after 3-Gy irradiation

Subcutaneous HT29 and HCT116 tumors were irradiated with 3 Gy, and the pO_2 distribution was imaged using EPRI 30 min, 60 min, and 24 h after irradiation (Figure 2A). The median pO_2 in the tumors represented the minimum values in the two strains 60 min after irradiation, and it was found to be lower in HCT116 than in HT29 (9.1 ± 1.5 vs. 14.0 ± 1.0 mmHg; $p = 0.045$) (Figure 2B).

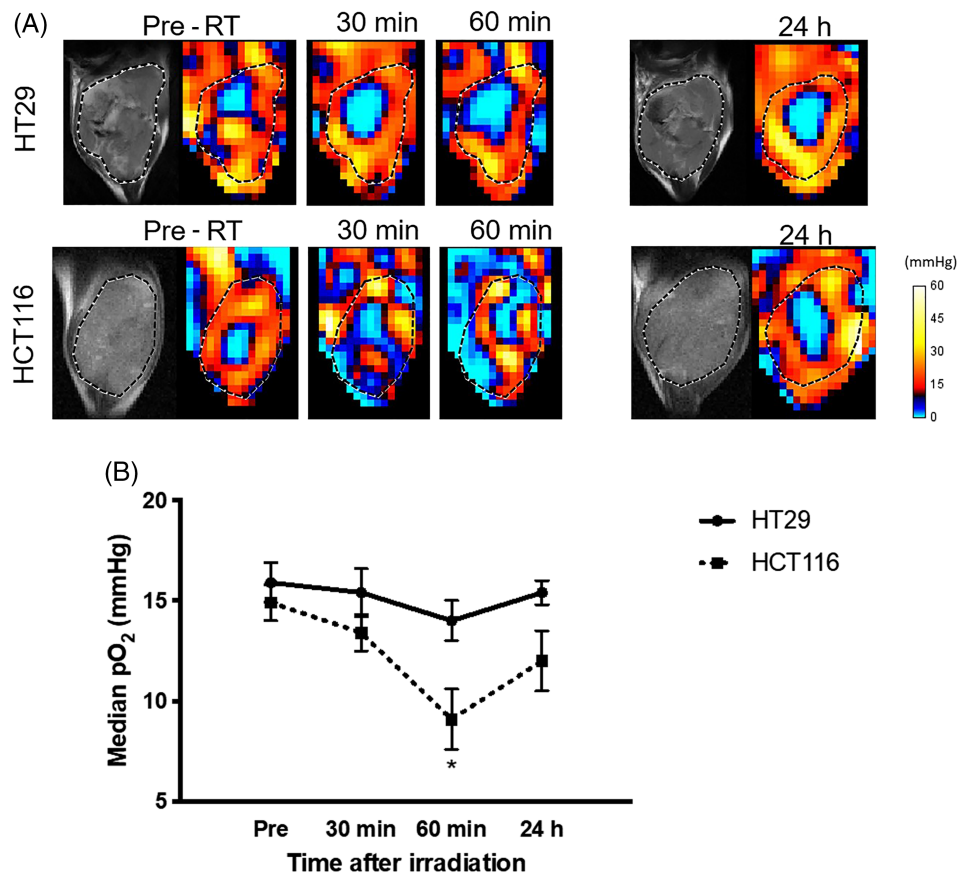


FIGURE 2 Strain dependence in transient hypoxia between HT29 and HCT116 tumors after 3-Gy irradiation. (A) Subcutaneous HT29 and HCT116 tumors ($n = 5$ in each group) were irradiated with 3 Gy, and the partial oxygen pressure (pO_2) distribution was imaged using electron paramagnetic resonance imaging 30 min, 60 min, and 24 h after irradiation. The reference T2WI-MR images are shown in the left panels. The tumors are outlined with black dotted lines. (B) The median pO_2 in the tumors represented the minimum values in the two strains 60 min after irradiation, and it was lower in the HCT116 than in the HT29 (9.1 ± 1.5 vs. 14.0 ± 1.0 mmHg, respectively; $p = 0.045$). *, statistically significant; RT, radiation therapy

3.3 | Redistribution of chronic and cycling hypoxia after irradiation

The distribution of pO_2 in the HT29 tumor was assessed using the EPRI datasets acquired before, 30 min, and 24 h after 3-Gy irradiation. Figure 3A shows the pO_2 images of the EPRI and the reference T2-weighted MR imaging before (left upper panel) and 24 h after irradiation (right upper panel), and the chronological transition of the pO_2 in representative areas with chronic and cycling hypoxia (lower panels). The proportion of normoxia remaining at pO_2 less than 10 mmHg throughout the timeframe between 30 and 60 min was 26.0%, which was significantly lower than that before irradiation (37.0%). By contrast, the proportions of chronic hypoxia and cycling hypoxia were elevated during this timeframe, although the trend was not statistically significant. The proportions of normoxia, chronic hypoxia, and cycling hypoxia were restored to the preirradiation state within 24 h (Figure 3B). Tumor size remained unchanged throughout the observation period.

4 | DISCUSSION

In this study, continuous EPRI demonstrated the reoxygenation process in tumor xenografts. The transient drop of pO_2 in the tumor after 3- to 20-Gy irradiation observed in this study was consistent with previously reported events where vascular obstruction attributable to microembolism and constriction was followed by reperfusion.²¹ It is noteworthy that the recovery of pO_2 24 h after irradiation was still incomplete, suggesting that the hypoxic region in the tumor might be increasing cumulatively during a series of daily fractionated radiation.

Previous studies have also demonstrated decreased oxygen pressure within a day following irradiation.²² Park et al. reviewed studies on radiation-induced vascular changes in human and experimental tumors, and proposed that vascular damage may induce tumor hypoxia after high dose-rate irradiation.²³ By contrast, Fujii et al.¹⁷ showed a rapid increase in SCC VII tumor oxygen levels within 12 h after irradiation. Another

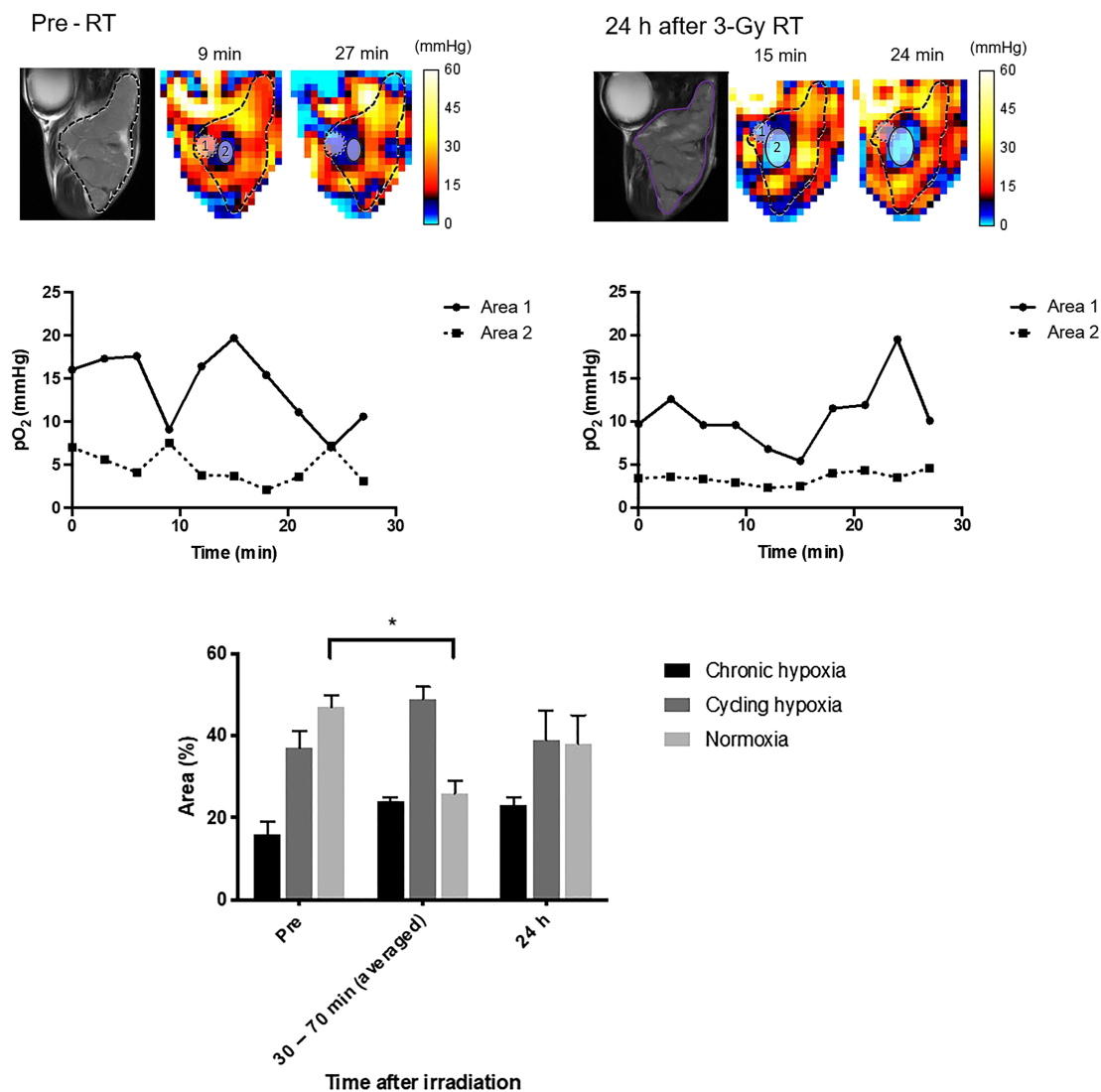


FIGURE 3 Redistribution of chronic and cycling hypoxia after irradiation. (A) The upper panels show the partial oxygen pressure (pO₂) images of the HT29 tumors on electron paramagnetic resonance imaging with the reference T2-weighted MR imaging before and 24 h after irradiation. The lower panels show the chronological transition of pO₂ in representative areas with chronic and cycling hypoxia. (B) The proportion of the normoxia with pO₂ > 10 mmHg throughout the timeframe (light gray) between 30 and 60 min was 26.0%, which was significantly lower than that before irradiation (37.0%). The proportions of chronic hypoxia (black) and cycling hypoxia (dark gray) were elevated in this timeframe, although these were not statistically significant (n = 5). *, statistically significant; RT, radiation therapy

study showed rapid reoxygenation in the C6 glioma within 24 h.²⁴ We considered that this discrepancy was due in part to the differences in basal oxygen levels in the tumors; the basal oxygen pressures were approximately 5 mmHg in the SCC VII and 5–9 mmHg in C6 glioma, whereas they were 16.2 and 14.9 mmHg in HT29 and HCT116 tumors, respectively. Yasui et al.²⁰ also showed that the number of pericytes covering blood vessels within SCC VII tumors was relatively small compared with that in HT29 tumors, which may contribute to the difference in O₂ diffusion. Collectively, we assume that radiation exposure may have two opposite directional effects on tumor oxygenation, one of which overrides the other and is dependent on the tumor-specific microenvironment, such as the vasculature extent, vascular bed characteristics, tumor oxygen consumption, and extent of immune response.^{25,26} Although the current study did not perform histopathological assessments that may correlate these responses with pO₂ alteration, this is worth investigating in future studies.

This study also demonstrated hypoxic areas with two distinct characteristics: areas with pO₂ less than 10 mmHg (chronic hypoxia) and those with pO₂ fluctuating across 10 mmHg (cycling hypoxia) in a cycle lasting several minutes, as reported by Yasui et al.²⁰ The phenomenon of cycling hypoxia has been investigated and found to be correlated with fluctuations in tumor perfusion, which was attributed to several factors including transient vasculature occlusion and narrowing.^{8,9}

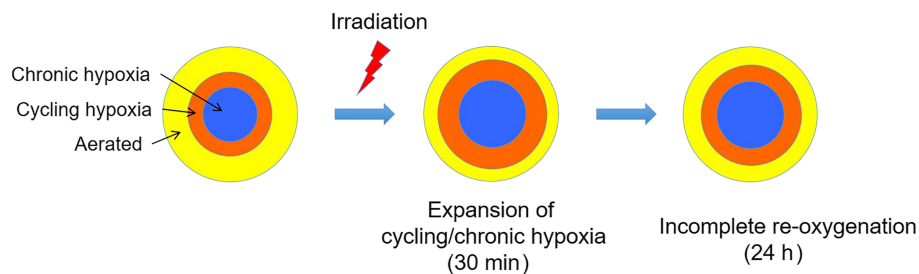


FIGURE 4 A schema of the biological effect of the radiation therapy against solid tumors considering cycling hypoxia in the reoxygenation process

EPRI studies showed that both the central chronic hypoxia and the peripheral cycling hypoxia expanded temporarily in the period between the 30- and the 60-min time points, followed by a reversal towards the preirradiation state within 24 h (Figure 3A). Indeed, although not statistically significant, both the regions of cycling and chronic hypoxia exhibited a tendency to expand from 30 to 60 min after irradiation, followed by a reduction in the area of cycling hypoxia and a less evident decrease in the area of chronic hypoxia (Figure 3B). The results of the single-dose irradiation study suggest that the biological effect of the multifractionated radiation therapy against solid tumors might be complicated, and cycling hypoxia should also be considered as a critical factor in the reoxygenation process (Figure 4).

Although much is still unknown regarding cycling hypoxia, we hypothesize that there are transitional zones in areas with cycling hypoxia in which the microvasculature adjacent to the chronic hypoxia or oxygenated areas is susceptible to radiation exposure. Some studies have revealed its contribution to the resistance against cancer treatment by not only decreasing the sensitivity of tumor cells to therapies, but also altering the microenvironment favorable for tumor progression and activating prosurvival pathways.^{22,27,28} Therefore, it is worth investigating the biological behavior of the cells that reside in the region with cycling hypoxia and its impact on the sensitivity to treatments, including radiation therapy. However, examining dynamic changes in the oxygen status of the tumor tissue is challenging because of the need for noninvasive *in vivo* experimental strategies that enable continuous evaluation with sufficient temporal and spatial resolutions.

Previous studies have successfully visualized oxygen distribution using MRI. Panek et al.²⁹ demonstrated spontaneous fluctuation of tissue oxygen levels using susceptibility mapping and dynamic contrast-enhanced studies. O'Connor et al.³⁰ utilized oxygen-enhanced MRI that uses the changes in the longitudinal relaxation of protons to monitor the oxygen concentration. Although these methods make use of conventional MRI apparatus, they provide a qualitative assessment of pO_2 in tumors. On the contrary, EPRI-oximetry provides quantitative measurement of the oxygen distribution with useful spatial and temporal resolution.^{20,31} The current study showed that cycling hypoxia was a substantial component of the postirradiation reoxygenation process contributing to the resistance to treatment. A limitation of this study is that it examined a short-term change in the oxygen distribution after single-dose irradiation. The longer-term observation of biological response to multifractionated irradiation also requires to be investigated for a more practical assessment of the tumor microenvironment during radiotherapy.

In conclusion, this is the first *in vivo* preclinical study to illustrate the chronological changes in the intratumoral environment with different oxygenation status in response to radiation therapy. EPRI successfully demonstrated the dynamic reoxygenation process in tumor xenografts after irradiation. Thus, EPRI can be utilized to develop new strategies for radiation therapy based on the concept of the reoxygenation process.

ACKNOWLEDGMENTS

This work was supported by grant 1ZIABC11692 from the National Institutes of Health, USA, and by grant 20H03628 and 20KK0253 from JSPS KAKEN Grants-in-Aid for Scientific Research.

DATA AVAILABILITY STATEMENT

The data that support the findings of this study are available from the corresponding author upon reasonable request.

ORCID

Tatsuya Kawai  <https://orcid.org/0000-0003-2572-3304>

REFERENCES

1. Rockwell S, Dobrucki IT, Kim EY, Marrison ST, Vu VT. Hypoxia and radiation therapy: past history, ongoing research, and future promise. *Curr Mol Med.* 2009;9:442-458. doi:10.2174/156652409788167087
2. Hockel M, Schlenger K, Aral B, Mitze M, Schaffer U, Vaupel P. Association between tumor hypoxia and malignant progression in advanced cancer of the uterine cervix. *Cancer Res.* 1996;1(56):4509-4515.

3. Dewhirst MW. Relationships between cycling hypoxia, HIF-1, angiogenesis and oxidative stress. *Radiat Res.* 2009;172:653-665. doi:[10.1667/RR1926.1](https://doi.org/10.1667/RR1926.1)
4. Van Putten LM, Kallman RF. Oxygenation status of a transplantable tumor during fractionated radiation therapy. *J Natl Cancer Inst.* 1968;40:441-451.
5. Howes AE. An estimation of changes in the proportions and absolute numbers of hypoxic cells after irradiation of transplanted C3H mouse mammary tumours. *Br J Radiol.* 1969;42:441-447. doi:[10.1259/0007-1285-42-498-441](https://doi.org/10.1259/0007-1285-42-498-441)
6. van Putten LM. Tumour reoxygenation during fractionated radiotherapy; studies with a transplantable mouse osteosarcoma. *Eur J Cancer.* 1968;4:172-182. doi:[10.1016/0014-2964\(68\)90015-7](https://doi.org/10.1016/0014-2964(68)90015-7)
7. Brown JM. Evidence for acutely hypoxic cells in mouse tumours, and a possible mechanism of reoxygenation. *Br J Radiol.* 1979;52:650-656. doi:[10.1259/0007-1285-52-620-650](https://doi.org/10.1259/0007-1285-52-620-650)
8. Chaplin DJ, Olive PL, Durand RE. Intermittent blood flow in a murine tumor: radiobiological effects. *Cancer Res.* 1987;47:597-601.
9. Kimura H, Braun RD, Ong ET, et al. Fluctuations in red cell flux in tumor microvessels can lead to transient hypoxia and reoxygenation in tumor parenchyma. *Cancer Res.* 1996;56:5522-5528.
10. Cairns RA, Kalliomaki T, Hill RP. Acute (cyclic) hypoxia enhances spontaneous metastasis of KHT murine tumors. *Cancer Res.* 2001;61:8903-8908.
11. Cairns RA, Hill RP. Acute hypoxia enhances spontaneous lymph node metastasis in an orthotopic murine model of human cervical carcinoma. *Cancer Res.* 2004;64:2054-2061. doi:[10.1158/0008-5472.CAN-03-3196](https://doi.org/10.1158/0008-5472.CAN-03-3196)
12. Cairns RA, Khokha R, Hill RP. Molecular mechanisms of tumor invasion and metastasis: an integrated view. *Curr Mol Med.* 2003;3:659-671. doi:[10.2174/1566524033479447](https://doi.org/10.2174/1566524033479447)
13. Krishna MC, Matsumoto S, Yasui H, et al. Electron paramagnetic resonance imaging of tumor pO₂. *Radiat Res.* 2012;177:376-386. doi:[10.1667/RR2622.1](https://doi.org/10.1667/RR2622.1)
14. Krishna MC, Subramanian S, Kuppusamy P, Mitchell JB. Magnetic resonance imaging for in vivo assessment of tissue oxygen concentration. *Semin Radiat Oncol.* 2001;11:58-69. doi:[10.1053/srao.2001.18104](https://doi.org/10.1053/srao.2001.18104)
15. O'Hara JA, Goda F, Liu KJ, Bacic G, Hoopes PJ, Swartz HM. The pO₂ in a murine tumor after irradiation: an in vivo electron paramagnetic resonance oximetry study. *Radiat Res.* 1995;144:222-229. doi:[10.2307/3579262](https://doi.org/10.2307/3579262)
16. Goda F, Bacic G, O'Hara JA, Gallez B, Swartz HM, Dunn JF. The relationship between partial pressure of oxygen and perfusion in two murine tumors after x-ray irradiation: a combined gadopentetate dimeglumine dynamic magnetic resonance imaging and in vivo electron paramagnetic resonance oximetry study. *Cancer Res.* 1996;56:3344-3349.
17. Fujii H, Sakata K, Katsumata Y, et al. Tissue oxygenation in a murine SCC VII tumor after x-ray irradiation as determined by EPR spectroscopy. *Radiother Oncol.* 2008;86:354-360. doi:[10.1016/j.radonc.2007.11.020](https://doi.org/10.1016/j.radonc.2007.11.020)
18. Matsumoto S, Hyodo F, Subramanian S, et al. Low-field paramagnetic resonance imaging of tumor oxygenation and glycolytic activity in mice. *J Clin Invest.* 2008;118:1965-1973. doi:[10.1172/JCI34928](https://doi.org/10.1172/JCI34928)
19. Matsumoto S, Yasui H, Mitchell JB, Krishna MC. Imaging cycling tumor hypoxia. *Cancer Res.* 2010;70:10019-10023. doi:[10.1158/0008-5472.CAN-10-2821](https://doi.org/10.1158/0008-5472.CAN-10-2821)
20. Yasui H, Matsumoto S, Devasahayam N, et al. Low-field magnetic resonance imaging to visualize chronic and cycling hypoxia in tumor-bearing mice. *Cancer Res.* 2010;70:6427-6436. doi:[10.1158/0008-5472.CAN-10-1350](https://doi.org/10.1158/0008-5472.CAN-10-1350)
21. Barker HE, Paget JT, Khan AA, Harrington KJ. The tumour microenvironment after radiotherapy: mechanisms of resistance and recurrence. *Nat Rev Cancer.* 2015;15:409-425. doi:[10.1038/nrc3958](https://doi.org/10.1038/nrc3958)
22. Michiels C, Tellier C, Feron O. Cycling hypoxia: A key feature of the tumor microenvironment. *Biochim Biophys Acta.* 2016;1866:76-86. doi:[10.1016/j.bbcan.2016.06.004](https://doi.org/10.1016/j.bbcan.2016.06.004)
23. Park HJ, Griffin RJ, Hui S, Levitt SH, Song CW. Radiation-induced vascular damage in tumors: implications of vascular damage in ablative hypofractionated radiotherapy (SBRT and SRS). *Radiat Res.* 2012;177:311-327. doi:[10.1667/RR2773.1](https://doi.org/10.1667/RR2773.1)
24. Hou H, Mupparaju SP, Lariviere JP, et al. Assessment of the changes in 9L and C6 glioma pO₂ by EPR oximetry as a prognostic indicator of differential response to radiotherapy. *Radiat Res.* 2013;179:343-351. doi:[10.1667/RR2811.1](https://doi.org/10.1667/RR2811.1)
25. Schae D, McBride WH. Links between innate immunity and normal tissue radiobiology. *Radiat Res.* 2010;173:406-417. doi:[10.1667/RR1931.1](https://doi.org/10.1667/RR1931.1)
26. Ozsoy HZ, Sivasubramanian N, Wieder ED, Pedersen S, Mann DL. Oxidative stress promotes ligand-independent and enhanced ligand-dependent tumor necrosis factor receptor signaling. *J Biol Chem.* 2008;283:23419-23428. doi:[10.1074/jbc.M802967200](https://doi.org/10.1074/jbc.M802967200)
27. Hsieh CH, Wu CP, Lee HT, Liang JA, Yu CY, Lin YJ. NADPH oxidase subunit 4 mediates cycling hypoxia-promoted radiation resistance in glioblastoma multiforme. *Free Radic Biol Med.* 2012;53:649-658. doi:[10.1016/j.freeradbiomed.2012.06.009](https://doi.org/10.1016/j.freeradbiomed.2012.06.009)
28. Tellier C, Desmet D, Petit L, et al. Cycling hypoxia induces a specific amplified inflammatory phenotype in endothelial cells and enhances tumor-promoting inflammation in vivo. *Neoplasia.* 2015;17:66-78. doi:[10.1016/j.neo.2014.11.003](https://doi.org/10.1016/j.neo.2014.11.003)
29. Panek R, Welsh L, Baker LCJ, et al. Noninvasive imaging of cycling hypoxia in head and neck cancer using intrinsic susceptibility MRI. *Clin Cancer Res.* 2017;23:4233-4241. doi:[10.1158/1078-0432.CCR-16-1209](https://doi.org/10.1158/1078-0432.CCR-16-1209)
30. O'Connor JPB, Boulton JKR, Jamin Y, et al. Oxygen-enhanced MRI accurately identifies, quantifies, and maps tumor hypoxia in preclinical cancer models. *Cancer Res.* 2016;76:787-795. doi:[10.1158/0008-5472.CAN-15-2062](https://doi.org/10.1158/0008-5472.CAN-15-2062)
31. Yasui H, Kawai T, Matsumoto S, et al. Quantitative imaging of pO₂ in orthotopic murine gliomas: hypoxia correlates with resistance to radiation. *Free Radic Res.* 2017;51:861-871. doi:[10.1080/10715762.2017.1388506](https://doi.org/10.1080/10715762.2017.1388506)

How to cite this article: Kawai T, Matsuo M, Takakusagi Y, et al. Continuous monitoring of postirradiation reoxygenation and cycling hypoxia using electron paramagnetic resonance imaging. *NMR in Biomedicine.* 2022;35(10):e4783. doi:[10.1002/nbm.4783](https://doi.org/10.1002/nbm.4783)